Optical and electrical measurements on electron beam evaporated CdTe thin films

M. M. ABD EL-RAHEEM[a,c*], H. M. ALI[b,c], N. M. EL-HUSAINY[a]
[a]*Physics Department, Faculty of Science, El-Taif University, K.S.A*
[b]*Physics Department, Faculty of Science, Al-Baha University, K.S.A*
[c]*Physics Department, Faculty of Science, 82524 Sohag, Sohag University, Egypt*

Thin films of CdTe with different film thickness have been grown on glass substrates with different film thickness by electron beam evaporation technique. The influences of the thickness and annealing temperature on the structural, optical and electrical characteristics of CdTe films have been investigated. The structure of the deposited CdTe films was of the zinc-blend type with a preferential orientation of (111) planes. The optical transmittance of these films was determined using a double beam spectrophotometer. All the spectra reveal interference fringes in the wavelength region from 820 to 2500 nm. The refractive index, n was calculated from the transmission spectra using the Swanepoel's method. The electrical resistivity measurements were carried out using the two-terminal configuration in air. High resistive CdTe films have been obtained after annealing at the temperature 400 ^oC.

(Received June 02, 2009; accepted June 15, 2009)

Keywords: Thin films, Structure properties, Transmittance, Refractive index, Electrical resistivity

1. Introduction

Cadmium Telluride is one of the promising semiconducting materials that have been studied for application in solar cells [1, 2], photorefractive devices, laser windows [3], infrared-, gamma-ray and x – ray detector [4]. CdTe has a direct band gap of 1.5 eV at room temperature and hence it is a suitable material for photovoltaic applications [5, 6].

The method of fabrication and properties of CdTe layer have great impact on the performance of the CdTe thin films solar cells. Major attention has been given in recent years to the investigation of electrical and optical properties of CdTe.

Many methods were used for the fabrication of CdTe layer such as close spaced sublimation [7, 8], electrodeposition [9], sputtering [10], close spaced vapor transport [11], spray pyrolysis [12], metalorganic chemical vapor deposition [13, 14] and vacuum evaporation [15]. The vacuum evaporation method has some advantages over other materials such as: the amount of impurities included in the growing layer can be minimized, the tendency to form oxides can be considerably reduced and the high degree of control is possible with electron beam sources, which provide efficient usage of evaporant and constant rate deposition [16, 17].

In the present work the effect of thickness and annealing temperature on the structural optical and electrical properties of CdTe thin films prepared by electron beam evaporation techniques has been investigated.

2. Experimental details

An ingot of CdTe crystal has been grown by the traveling heater method THM. The starting materials consisted of 50% atomic weight of cadmium and tellurium of 99.999% purity. For the removal of surface oxides, Cd and Te were etched by HCl and HNO_3, respectively and then washed many times in distilled and deionized water. The materials were then charged into a silica tube lined with pyrolytic graphite, and then evacuated down to 10^{-6} torr and then sealed off. The ampoule (which was tapered to a point at the bottom of the ampoule to encourage the nucleation of a single crystal) was put in a furnace. The temperature of the furnace was raised gradually to 500 ^oC and was kept constant for two hours. After that the temperature was raised to 850 ^oC gradually and was fixed for three hours, then elevating the temperature gradually to 1092 ^oC, during which the furnace was rocked slowly. The temperature of the furnace was kept constant at 1092 ^oC for 12 hours and cooled down slowly. For purification, zone refining step was used as follows, the resultant CdTe charge was put into another graphitized tube containing 3 g of Te at the bottom, where Te was used as an impurity scavenger. The lower end of the tube is inserted into the working coil of an induction furnace (Model 50, 1 kW at 450 kHz) and lowered through the working coil at a rate 5 mm/hr. After the zone refining step, CdTe charge was again inserted into a third coated silica tube, which is tapered to a point at the bottom of the ampoule. The ampoule is again evacuated down to 10^{-6} torr and sealed off and lowered in a furnace at 750 ^oC at a rate of 2 mm a day.

Thin films of CdTe were fabricated by the electron beam evaporation technique onto ultrasonically cleaned microscope glasses using an Edwards model E306A high vacuum coating unit at pressures of 10^{-3} Pa. The deposition rate was 8-10 Å/s. The film thickness was determined by means of a Maxtek model TM200 digital film thickness monitor.

Investigations of the microstructure were carried out using a Cu Kα x-ray diffractometer (Philips model PW1710, Holland; λ = 1.541 838 ° A). The compositional analysis of CdTe bulk material was studied by the energy dispersive analysis of X-rays (EDAX) (Jeol JSM-5300, Japan).

A Jasco V-570 UV–visible–NIR spectrophotometer (with photometric accuracy of ±0.002–0.004 absorbance and ±0.3% transmittance) was employed to record the transmission spectra over the wavelength range 200–2500 nm at normal incidence. Transmission spectra were taken at normal incidence with reference to air. The cross-section of the incident light was minimized using a suitable mask to eliminate the effects of layer inhomogeneities.

The electrical resistivity measurements were carried out using the two-terminal configuration by applying constant voltage to the sample and measuring the current through it using Keithley 614 electrometer.

The annealing temperature of the deposited films was carried out at fixed temperature of 250 and 400 ^oC for 30 minute in a fully controlled furnace in air.

3. Results and discussion

Fig. 1(a), (b) and (c) shows the typical x-ray diffraction (XRD) spectra obtained from CdTe films of as deposited and annealed at 250 ^oC and 400 ^oC for 30 minute in air respectively for different film thicknesses. The structure of the deposited CdTe films was of the zinc-blend type with a preferential orientation of the (111) planes. For as deposited films, one diffraction peak can be observed at 23.75^o which corresponds to the cubic (111) orientation.

The intensity of the (111) peak increases with increasing the film thickness from 0.8 to 1.8 µm. All the films annealed at 250 and 400 ^oC showed preferential growth of the film crystallites corresponding to the (111), (220), (311) and (422) planes with the peak positions at 2θ=23.75°, 39.31°, 46.4° and 71.21° respectively. The peaks corresponding to the (220), (311) and (422) planes are of a very small intensity compared with that of the (111) plane. The intensity of all diffraction peaks increase strongly after increasing the temperature of annealing to 250 ^oC. After annealing at 400 °C (Fig. 1-c) the (111) peak intensity decreases when compared with the same peak in Fig. 1 (a) and (b), indicating a randomization due to the appearance of (220) and (311) oriented grains at the expense of the (111) grains [18].

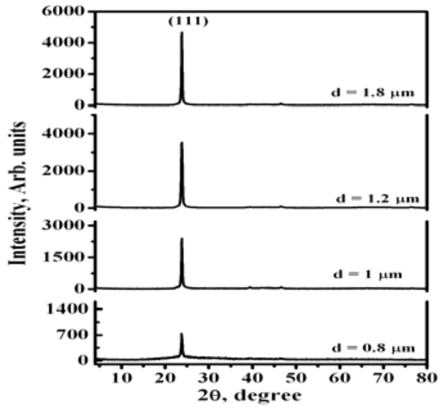

(a)

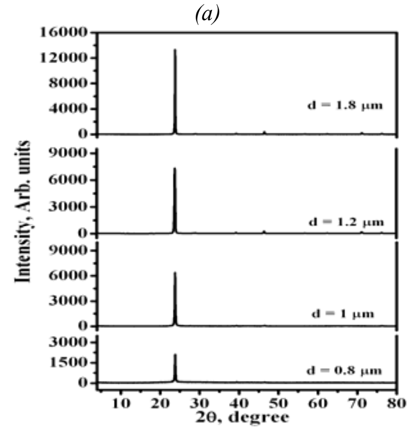

(b)

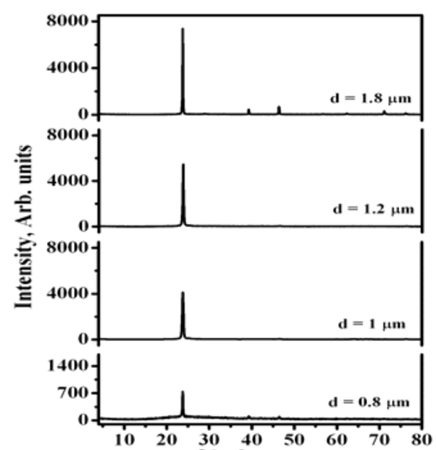

(c)

Fig.1. X-ray diffraction patterns of as deposited CdTe thin film (a) and annealed at different temperatures of 250 ^oC (b) and 400 ^oC (c) as a function of film thickness.

On the other hand, the full width at half maximum (FWHM) decreases with increasing the temperature of annealing and film thickness, indicating an increase of the grain size with increasing the annealing temperature and/or film thickness as shown in Fig. 2 (a).

Using the average FWHM of the preferred line, the grain size, D, has been calculated according to the Scherrer formula:

$$D = \frac{0.9\lambda}{B\cos\theta_B} \tag{1}$$

Here, λ = 1.54056 Å, θ_B is the diffraction angle and B is the measured broadening of the diffraction line peak at an angle of 2θ, at half its maximum intensity (FWHM), corrected for the instrumental effects.

The calculated grain sizes of the as deposited and annealed films are plotted as a function of the film thickness as shown in Fig. 2 (b). The latter figure suggests that the grain size increases with increasing the film thickness for both as deposited and annealed films. On the other hand, a very small difference between the grain size of the annealed film at 250 and 400 °C were observed.

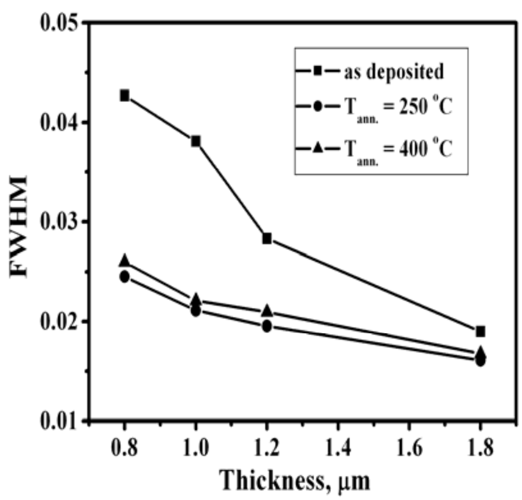

(a)

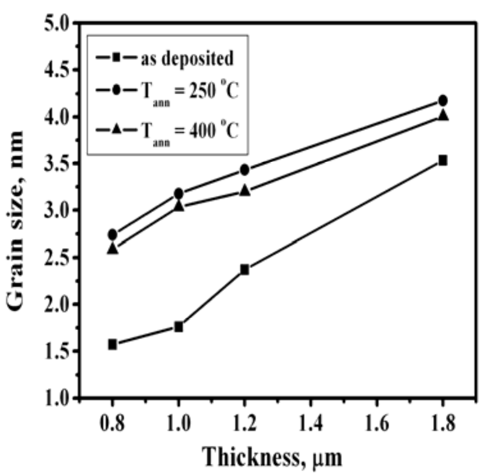

(b)

Fig. 2. The variation of (a) FWHM of the (111) CdTe peak and (b) the grain size of CdTe with the film thickness for as deposited and annealed films.

The dislocation density (φ) was evaluated using the formula suggested by Williamson and Smallman [19], which is $\varphi = n/D^2$. On the other hand, for minimum dislocation density n = 1. As shown in Fig. 3 the dislocation density decreases with increasing the film thickness, which can be ascribed to the improvement of the film crystallinity.

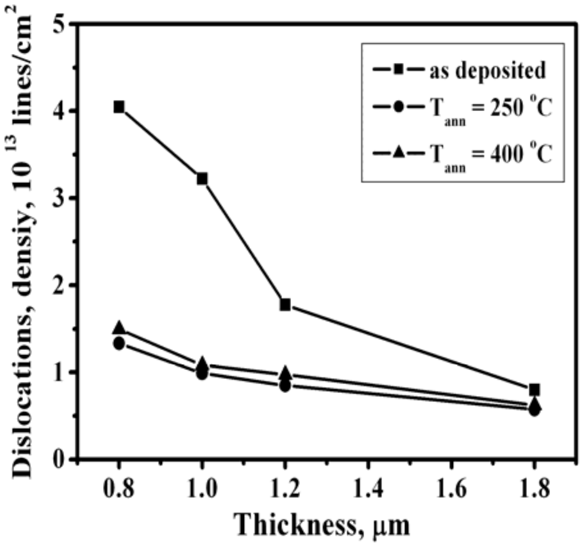

Fig. 3. The variation of the dislocation density of CdTe with the film thickness for as deposited and annealed films.

Fig. 4 shows the optical transmittance spectrum of as grown and annealed CdTe films in the wavelength range 200–2500 nm for different film thickness. An excellent surface quality and homogeneity of the film were confirmed from the appearance of interference fringes in the transmission spectra. All the spectra reveal interference fringes in the wavelength regions from 820 to 2500 nm. It is clear that the films with 1µm or greater absorbs 100% of the incident light in the solar spectrum region. It is observed also that the number of fringes increases as the film thickness increases, whereas the transmittance decreases with increasing annealing temperature. It is noticed that, in the weak absorption, sharp interference fringes appeared and indicated that the air/layer and layer/glass interfaces are flat and parallel [20]. The decrease of the transmittance with increasing temperature of annealing may be due to the improvement of film crystallinity and/or the increase of the grain size.

Strong absorption was observed at photon energies 1.52, 1.49, 1.49 and 1.45 eV for the thicknesses 0.8, 1, 1.2 and 1.8 µm respectively, where interference effects are suppressed almost completely due to a well defined band edge. Residual absorption at lower photon energies is more probably due to other defects and impurities arising from the vacuum environment and glass substrate.

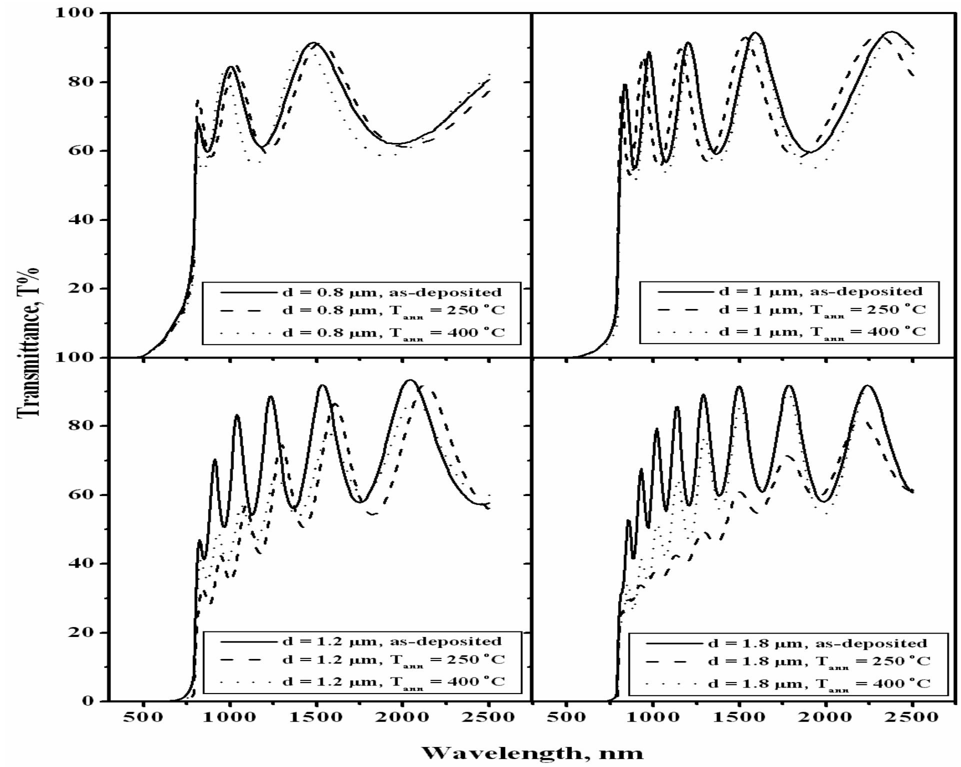

Fig. 4. Optical transmittance spectra of as deposited and annealed CdTe films with different film thickness as a function of wavelength.

The refractive index, n was calculated from the transmission spectra using Swanepoel's method [21, 22] using the envelope method suggested by Manifacier et al. [23]. The envelopes connecting the interference maxima and minima are considered to be continuous functions of the wavelength. Therefore, for each maximum of the transmittance curves, T_M, a corresponding minimum, T_m, may be determined at the same wavelength, λ. The refractive index of CdTe thin films, *n*, as a function of wavelength, λ; can be calculated using the following equations [21-24]:

$$n = \sqrt{N + \sqrt{(N^2 - s^2)}} \tag{2}$$

where *N* and *s* are given by

$$N = \frac{1+s^2}{2} + \frac{2s(T_M - T_m)}{T_M T_m} \tag{3}$$

The refractive index of the substrate *s* could be calculated from the following formula

$$s = \frac{1}{T_s} + \left(\frac{1}{T_s} - 1\right)^{1/2} \tag{4}$$

where T_s is the transmission of the substrate.

Fig. 5 shows the thickness dependence of the refractive index for as deposited and annealed films at 250 and 400 ^oC. It was found that the refractive index increases with increasing the film thickness for both as deposited and annealed films which can be attributed to the increase of the packing density of the films and the improvement of the films crystallinity [25, 26]

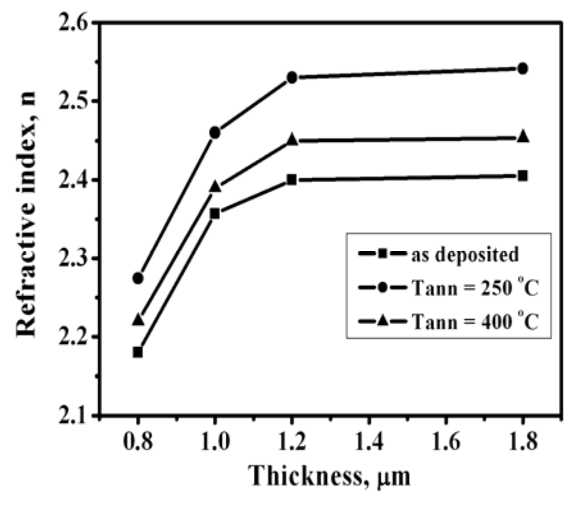

Fig. 5. Thickness dependence of refractive index of as deposited and annealed films at 250^{o}C and 400 ^{o}C.

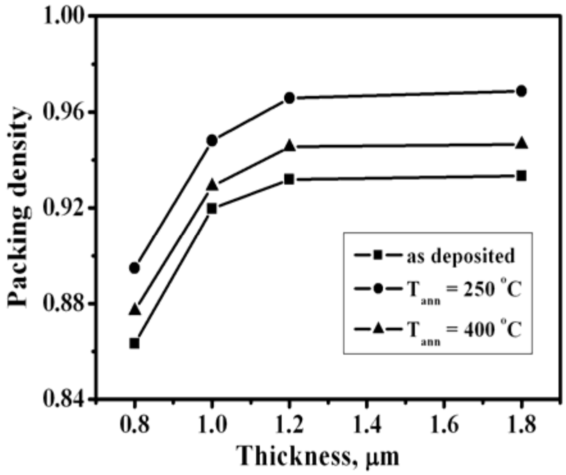

Fig. 6. Variation of packing density with film thickness for as deposited and annealed films at 250 and 400 °C

The packing density of the film can be estimated from the following eqn. [27]:

$$n_f^2 = \frac{(1-p)\,n_v^4 + (1+p)\,n_v n_s^2}{(1+p)\,n_v^2 + (1-p)\,n_s^2} \tag{5}$$

where n_f is the refractive index of a composite film, n_s is the index of the solid material of the film (single crystal value), n_v is the index of the void in the film (equals one for air), and p is the packing density. The behaviour of the packing densities with respect to the film thickness for as deposited and annealed films is shown in Fig. 6. It has been found that the calculated packing density values increase with increasing the film thickness.

Using the optical absorption coefficient α evaluated from the optical transmission data, the allowed direct band gap E_g values were obtained by extrapolating the linear part of the plots of $(ah\nu)^2$ versus the photon energy ($h\nu$) to $\alpha = 0$. The corresponding band gaps of CdTe films are shown in Fig. 7.

As seen in this figure the energy gap gradually decrease from 1.55 to 1.45 eV with increasing either the film thickness or annealing temperature. The decrease of the optical energy gap can be, in general, correlated with the increase of the absorbance as a result of increasing the film crystallinity due to the increase of the grain size.

The short wave cutoff wavelength has been determined using the following equation

$$\lambda_{cutoff}(\mu m) = \frac{1.24}{E_g(eV)} \tag{6}$$

where E_g is the energy band gap of the material. The cutoff wavelength is directly affected by the energy gap of the material [28, 29]. According to the decrease in the optical band gap, the short wave cutoff wavelength increases, as shown in Fig. 8.

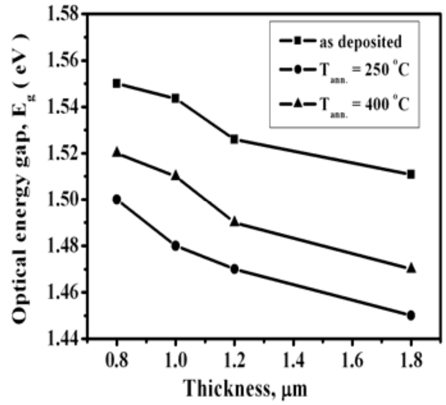

Fig. 7. Variation of optical energy gap with film thickness for as deposited and annealed films at 250 and 400 °C.

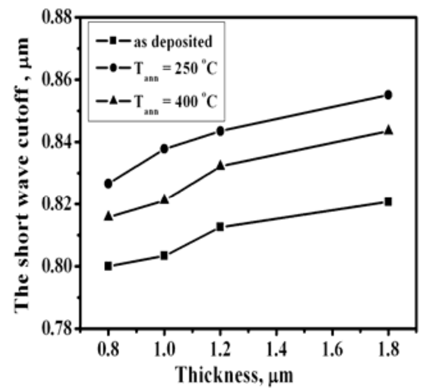

Fig. 8. The short wave cutoff dependence of film thickness for as deposited and annealed films at 250 °C and 400 °C.

The electrical properties of CdTe films is an important factor for the performance of CdTe solar cells. The thickness dependence of the electrical resistivity of as deposited and annealed films is shown in Fig. 9.

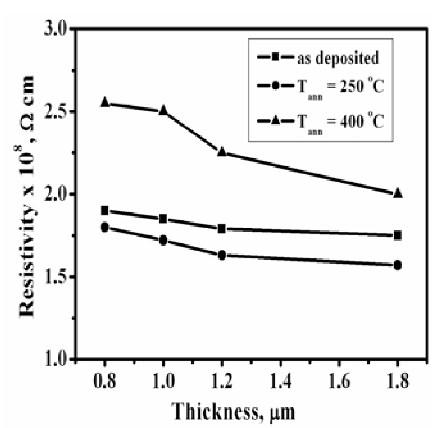

Fig. 9. Variation of the electrical resistivity with film thickness for as deposited and annealed films at 250 and 400 °C.

It can be seen that all films exhibit a resistivity of 10^8 Ω cm. The high value of the electrical resistivity can probably be attributed to the stoichiometric behaviour of films. Small variation in the resistivity value is observed with increasing the film thickness from 0.8 to 1.8 μm. The electrical resistivity of the films found to decrease with annealing up to 250 ^oC which may be attributed to grain growth and possibly recrystallization [30]. On the other hand, the resistivity increased with increasing the annealing temperature at 400 °C due to the randomization as a result of appearance of (220) and (311) oriented grains at the expense of the (111) grains.

4. Conclusions

The influence of thickness and annealing temperature on the structural, optical and electrical characteristics of CdTe films deposited by electron beam evaporation technique has been investigated. The structure of the deposited CdTe films was of the zinc-blend type with a preferential orientation of (111) planes. The optical transmittance of these films revealed interference fringes in the wavelength regions from 820 to 2500 nm. It was found that the films with 1μm or greater, absorbs 100% from the incident light in the solar spectrum region. The refractive index was calculated from the transmission spectra using the Swanepoel's method. Values of the refractive index were in the range of 2.18 to 2.54. The electrical resistivity measurements were carried out using the two-terminal configuration in air. High resistive CdTe films have been obtained after annealing temperature at 400 ^oC. The behavior of the annealed CdTe films at 400 ^oC makes it useful for gamma detection devices and as a resistive-absorber layer for solar cells.

References

[1] T. Aramoto, S Kumazawa, H. Higuchi, T. Arita, S. Shibutani, T. Nishio, J. Nakajima, A. Tsuji, M. Hanafusa., T. Hobino, K. Omura, H. Ohyama, M. Murozono, Japanese J. of Applied Physics **36**, 6304 (1997).

[2] A. Bosio, N. Romeo, S. Mazzamuto, V. Canevari, Progress in Crystal Growth and Characterization of Materials **52**, 247 (2006).

[3] V. Popovych, I. Virt, F. Sizov, V. Tetyorkin, Z. Tsybrii, L. Darchuk, O. Parfenjuk, M. Ilashchuk, J. of Crystal Growth **308**, 63 (2007).

[4] M. Burgelman, J. Verschraegen, S. Degrave, P. Nollet, Thin solid films **480-481**, 392 (2005).

[5] T. Razykov, G. Contreras-Puente, G. Chornokur, M. Dybjec, Yu. Emirov, B. Ergashev, C. Ferekides, A. Hubbimov, B. Ikramov, K. Kouchkarov X., Mathew, D. Morel, S. Ostapenko, E. Sanchez-Meza, E. Stefanakos, H. Upadhyaya, O.Vigil-Galan, Yu. Vorobiev, Solar Energy **83**, 90 (2009).

[6] S. Lalitha, S. Karazhanov, P. Ravindran, S. Senthilarasu, R. Sathyamoorthy, J. Janabergenov, Physica B **387**, 227 (2007).

[7] J. Britt, C. Ferekides, Appl. Phys. Lett. **62**, 2851 (1993).

[8] X. Wu, J. C. Keane, C. DeHart, D. S Albin, A. Duda, T. A. Gessert, S. Asher, D. H Levi, P. Scheldon, Proc. 17th European Photovoltaic Solar Energy Conference, Munich, Germany, 995 (2001).

[9] M. Miyake, K. Murase, T. Hirato, Y. Awakura, J. Electroanal. Chem. **562** (2), 247 (2004).

[10] A. Gupta, A. D. Compaan, In: Materials Research Society Symposium – Proceed- ings **763**, 161 (2003).

[11] R. Mendoza-Pérez, G. Santana-Rodríguez, J. Sastre-Hernández, A. Morales-Acevedo, A. Arias-Carbajal, O. Vigil-Galan, J. C. Alonso, G. Contreras-Puente, Thin Solid Films **480–481**, 173 (2005).

[12] K. Vamsi Krishna V. Dutta, J. Appl. Phys. **96** (7), 3962 (2004).

[13] A. Hartley, S. J. C. Irvine, D. P. Halliday, M. D. G. Potter, Thin Solid Films **387**(1–2), 89 (2001).

[14] Z. C. Feng, H. C. Chou, A. Rohatgi, G. K. Lim, A. T. S. Wee, K. L. Tan, J. Appl. Phys. **79**(N4), 2151 (1996).

[15] S. Chandramohana, R. Sathyamoorthy, P. Sudhagar, D. Kanjilal, D. Kabiraj, K. Asokan, Thin Solid Films **516**, 5508 (2008).

[16] U. Khairnar, D. Bhavsar, R. Vaidya, G. Bhavsar, Mater. Chem. Phys. **80**, 421 (2003).

[17] H. M. Ali, H. A. Abd El-Ghanny, J. Phys.: Condens. Matter. **20**, 155205 (2008).

[18] E. Bacaksiz, B. M. Basol, M. Altunbaş, V. Novruzov, E. S. Yanmaz, Nezir, Thin Solid Films **515**, 3079 (2007).

[19] G. Williamson, R. Smallman, Phil. Mag. **1**, 34 (1956).

[20] B. Zengir, M. Bayhan, S. Kavasouglu, J. of Arts and sciences Sayt: **5**, Mayts 2006.

[21] R. Swanepoel, J. Phys. E: Sci. Instrum. **16**, 121 (1983).

[22] R. Swanepoel, J. Phys. E: Sci. Instrum. **17**, 896 (1984).

[23] J. C. Manifacer, J. Gasiot, J. P. Fillard, J. Phys. E: Sci.Instrum. **9**, 1002 (1976).

[24] E. R Shaaban, N. El-Kabnay, A. M. Abou-sehly, N. Afify, Physica B **381**, 24 (2006).

[25] H. M. Ali, M. M. Abd El-Raheem, N. M. Megahed, H. A. Mohamed, J. of Physics and Chemistry of Solids **67**, 1823 (2006).

[26] T. K. Subramanyam, G. Mohan Rao, S. Uthanna, Materials Chemistry and Physics **69**, 133 (2001).

[27] H. A. Macleod, J. Vac. Sci. Technol. A **4**, 418 (1986).

[28] S. A. Knickerbocker, A. K. Kulkarni, Acad. J. Sci. Technol. A **14**(3), 1709 (1996).

[29] H. M. Ali, Phys. Stat. Sol. (a) **202**(14), 2742 (2005).

[30] O. Vigil, F. Cruz, A. Morales-Acevedo, G. Contreras-Puente, L. Vaillant, G. Santana, Materials Chemistry and Physics **68**, 249 (2001).

*Corresponding author: elneh@yahoo.com